The serum- and glucocorticoid-inducible kinase 1 (SGK1) influences platelet calcium signaling and function by regulation of Orai1 expression in megakaryocytes

Oliver Borst,[1,2] Eva-Maria Schmidt,[1] Patrick Münzer,[1] Tanja Schönberger,[2] Syeda T. Towhid,[1] Margitta Elvers,[2] Christina Leibrock,[1] Evi Schmid,[1] Anja Eylenstein,[1] Dietmar Kuhl,[3] Andreas E. May,[2] Meinrad Gawaz,[2] and Florian Lang[1]

[1]Department of Physiology, University of Tübingen, Tübingen, Germany; [2]Innere Medizin III, Department of Cardiology and Cardiovascular Medicine, University of Tübingen, Tübingen, Germany; and [3]Center for Molecular Neurobiology, Institute for Molecular and Cellular Cognition, University Medical Center Hamburg-Eppendorf, Hamburg, Germany

Platelets are activated on increase of cytosolic Ca^{2+} activity ($[Ca^{2+}]_i$), accomplished by store-operated Ca^{2+} entry (SOCE) involving the pore-forming ion channel subunit Orai1. Here, we show, for the first time, that the serum- and glucocorticoid-inducible kinase 1 (SGK1) is expressed in platelets and megakaryocytes. SOCE and agonist-induced $[Ca^{2+}]_i$ increase are significantly blunted in platelets from SGK1 knockout mice ($sgk1^{-/-}$). Similarly, Ca^{2+}-dependent degranulation, integrin $\alpha_{IIb}\beta_3$ activation, phosphatidylserine exposure, aggregation, and in vitro thrombus formation were significantly impaired in $sgk1^{-/-}$ platelets, whereas tail bleeding time was not significantly enhanced. Platelet and megakaryocyte Orai1 transcript levels and membrane protein abundance were significantly reduced in $sgk1^{-/-}$ mice. In human megakaryoblastic cells (MEG-01), transfection with constitutively active ^{S422D}SGK1 but not with inactive ^{K127N}SGK1 significantly enhanced Orai1 expression and SOCE, while effects reversed by the SGK1 inhibitor GSK650394 (1μM). Transfection of MEG-01 cells with ^{S422D}SGK1 significantly increased phosphorylation of IκB kinase α/β and IκBα resulting in nuclear translocation of NF-κB subunit p65. Treatment of ^{S422D}SGK1-transfected MEG-01 cells with the IκB kinase inhibitor BMS-345541 (10μM) abolished SGK1-induced increase of Orai1 expression and SOCE. The present observations unravel SGK1 as novel regulator of platelet function, effective at least in part by NF-κB–dependent transcriptional up-regulation of Orai1 in megakaryocytes and increasing platelet SOCE. (*Blood*. 2012;119(1):251-261)

Introduction

Platelet adhesion, activation, and aggregation are essential for primary hemostasis at sites of vascular injury but are also critically important for the development of acute thrombotic occlusion at regions of atherosclerotic plaque rupture, the major pathophysiologic mechanism underlying myocardial infarction and ischemic stroke.[1]

Platelet activation is triggered by various agonists, including subendothelial collagen, ADP released from activated platelets, thrombin generated by the coagulation cascade, or the collagen receptor glycoprotein VI (GPVI)–specific agonists convulxin (CVX) and collagen-related peptide (CRP).[2] The agonists lead to platelet granule release, integrin $\alpha_{IIb}\beta_3$ activation, phosphatidylserine exposure, aggregation, and thrombus formation.[2] All those platelet responses depend on an increase of cytosolic Ca^{2+} concentration ($[Ca^{2+}]_i$),[3,4] which is accomplished by inositol-1,4,5-triphosphate-mediated Ca^{2+} release from intracellular stores triggering subsequent stimulation of store-operated Ca^{2+} entry (SOCE) across the plasma membrane.[5] Two key players in platelet SOCE have recently been identified: The 4-transmembrane-spanning pore-forming calcium release-activated channel moiety Orai1, which mediates entry of extracellular Ca^{2+}, and stromal interaction molecule 1 (STIM1), an Orai1 regulating Ca^{2+} sensor expressed predominantly in the endoplasmic reticulum.[6-8] Regulators of

Orai1 in other cell types include receptor for activated protein kinase C-1,[9] reactive oxygen species,[10] and lipid rafts.[11]

However, regulation of Orai1 in platelets is poorly understood. Platelet activation has been shown to be regulated in vitro and in vivo by the PI3K/Akt signaling cascade.[12,13] Interference with PI3K signaling has previously been shown to compromise Ca^{2+} influx into platelets.[14,15]

Signaling molecules regulated by PI3K signaling include the serum- and glucocorticoid-inducible kinase 1 (SGK1), a kinase belonging to the AGC family of serine/threonine protein kinases.[16,17] SGK1 has originally been cloned as a glucocorticoid-sensitive gene but later shown to be regulated by a variety of hormones and other triggers, including thrombin, growth factors IGF-1 and TGF-β, oxidative stress, and ischemia.[17]

SGK1 has previously been reported to regulate a wide variety of carriers and ion channels, including the epithelial Ca^{2+} channels TRPV5 and TRPV6.[17] Most recently, SGK1 has been shown to be critically important for the Ca^{2+} entry into mast cells after activation of the IgE receptor,[18] an effect mediated by regulation of Orai1.[19] Furthermore, SGK1 participates in the regulation of renal tubular Na^+ reabsorption, salt appetite, and thus blood pressure.[17] A gain-of-function SGK1 gene variant, the combined presence of single nucleotide polymorphism in intron 6 (rs1743966) and in exon 8 (rs1057293), is associated with enhanced blood pressure.[20]

The same genetic SGK1 variants are associated with ischemic stroke, an association partially independent of blood pressure, and thus the result of additional SGK1-dependent mechanisms.[21]

SGK1 has been shown to foster coagulation by up-regulation of tissue factor expression.[22] But prothrombotic activity is in addition critically dependent on the function of platelets, key players in the initiation of arterial thrombosis and vascular occlusion resulting in ischemic diseases.[23] Surprisingly, nothing is hitherto known about the influence of SGK1 on platelet function.

Thus, the present study explored the role of SGK1 in the regulation of platelet function. We could show, for the first time, that SGK1 is strongly expressed in platelets and megakaryocytes, acts as an important regulator of NF-κB–dependent Orai1 expression in megakaryocytes, and thus influences Ca^{2+} response, activation, and thrombus formation of released platelets.

Methods

Chemicals and antibodies

Platelets were activated using ADP (Sigma-Aldrich), thrombin (Roche Diagnostics), CVX (Enzo), collagen (Nycomed), CRP (Richard Farndale, University of Cambridge, United Kingdom), and thrombin receptor agonist PAR-4 activating peptide (NH2-AYPGKF, JPT Peptide Technologies). Fluorophore-labeled antibodies anti–P-selectin-FITC (Wug.E9-FITC; Emfret Analytics), anti–integrin $\alpha_{IIb}\beta_3$-PE (JON/A-PE; Emfret Analytics), and annexin V–Fluos (Roche Diagnostics) were used for flow cytometric analysis.

Preparation of human platelets

Blood from healthy volunteers was collected in ACD buffer and centrifuged at 200g for 20 minutes. The obtained platelet-rich plasma was added to modified Tyrode-HEPES buffer (137mM NaCl, 2.8mM KCL, 12mM $NaHCO_3$, 5mM glucose, 0.4mM Na_2HPO_4, 10mM HEPES, 0.1% BSA, pH 6.5). After centrifugation at 900g for 10 minutes and removal of the supernatant, the resulting platelet pellet was resuspended in Tyrode-HEPES buffer (pH 7.4, supplemented with 1mM $CaCl_2$).

Cell culture and transfection

The human megakaryoblastic leukemia cell line MEG-01 (DSMZ) was cultured in RPMI 1640 medium with Glutamax (Invitrogen), 10% FBS (Invitrogen), and 1% penicillin/streptomycin (Invitrogen) in a humidified atmosphere at 37°C and 5% CO_2. MEG-01 and human embryonic kidney (HEK293) cells were transiently transfected for 48 hours with the constitutively active SGK1 mutant ^{S422D}SGK1 (hSGK1^{SD} in pCDNA3.1), which does not require activation by phosphoinositide-dependent kinase PDK1,[19] or the inactive mutant ^{K127N}SGK1 (hSGK1^{KN} in pCDNA3.1), which lacks catalytic activity.[19] Transfections were performed as described previously[24] using FuGENE HD transfection reagent (Roche Diagnostics) according to the manufacturer's instructions. For experiments with pharmacologic inhibition of SGK1 or IκB kinase (IKK), 1μM GSK650394 (Solvay) or 10μM BMS-345541 (Sigma-Aldrich) was added.

Mice

Gene-targeted mice lacking functional SGK1 ($sgk1^{-/-}$) and the corresponding wild-type littermate mice ($sgk1^{+/+}$) were generated and bred as described by Wulff et al.[25] Animals were genotyped by PCR. All animal experiments were conducted according to German law for the welfare of animals and were approved by local authorities.

Preparation of mouse platelets

Platelets were obtained from 10- to 12-week-old $sgk1^{-/-}$ mice and $sgk1^{+/+}$ mice of either sex. The mice were anesthetized with ether, and blood was drawn from the retro-orbital plexus into heparinized tubes. Blood parameters were analyzed with pocH-100iv automatic hematology analyzer (Sysmex). Platelet-rich plasma was obtained by centrifugation at 260g for 5 minutes. Afterward, platelet-rich plasma was centrifuged at 640g for 5 minutes to pellet the platelets. To ease platelets, apyrase (0.02 U/mL, Sigma-Aldrich) and prostaglandin I_2 (0.5μM, Calbiochem) were added to the platelet-rich plasma. After 2 washing steps, the pellet of washed platelets was resuspended in modified Tyrode-HEPES buffer (pH 7.4, supplemented with 1mM $CaCl_2$).

Isolation and culture of murine megakaryocytes

For the isolation of murine $sgk1^{-/-}$ and $sgk1^{+/+}$ megakaryocytes, bone marrow cells were harvested by flushing the femurs and tibiae with PBS as described by Shivdasani and Schulze.[26] The obtained cells were separated over Percoll (GE Healthcare) and cultured in specific growth medium (MethoCult; StemCell Technologies) containing 50 ng/mL thrombopoietin (Invitrogen) as described previously.[27] After 5 to 7 days, differentiation into megakaryocytes was tested by microscopy and glycoprotein Ib (GPIb) staining.

RT-PCR analysis

To determine SGK1 and Orai1 mRNA abundance in platelets and megakaryocytes from $sgk1^{-/-}$ and $sgk1^{+/+}$ mice as well as in MEG-01 cells, mRNA was extracted and quantitative real-time PCR was performed as described in supplemental Methods (available on the *Blood* Web site; see the Supplemental Materials link at the top of the online article).

Flow cytometry

Two-color analysis of mouse platelet activation was conducted using fluorophore-labeled antibodies for P-selectin expression (Wug.E9-FITC) and the active form of $\alpha_{IIb}\beta_3$ integrin (JON/A-PE). Heparinized whole blood was diluted 1:20 in modified Tyrode buffer and washed twice. After adding 1mM $CaCl_2$, blood samples were mixed with antibodies and subsequently stimulated with agonists for 15 minutes at room temperature. For analysis of phosphatidylserine exposure, washed platelets were diluted in Tyrode buffer containing 2mM $CaCl_2$ and activated with CVX and/or thrombin for 15 minutes and stained with annexin V–Fluos at room temperature. For measuring Orai1 surface expression, washed platelets were incubated for 60 minutes (37°C) with Orai1 rabbit anti–mouse antibody (Proteintech), washed once in PBS, and stained in 1:500 diluted FITC-labeled goat anti–rabbit secondary antibody (Invitrogen) for 30 minutes (37°C). In all approaches, reaction was stopped by addition of PBS and samples were immediately analyzed on a FACSCalibur flow cytometer (BD Biosciences).

Platelet aggregometry

Aggregation experiments were performed in diluted whole blood with electrode impedance aggregometry (Model 700; Chrono-Log). Citrate-anticoagulated whole blood was diluted with physiologic saline. After calibration, agonists were added at the indicated concentrations and aggregation was measured for 10 minutes with a stir speed of 1000 rpm at 37°C. The extent of aggregation was quantified in ohms (Ω) by comparing the deflection of the trace with the calibration mark representing 20 Ω. The data analysis was performed with AGGRO/LINK8 software (Chrono-Log).

Calcium measurements

Washed murine platelets were suspended in Tyrode buffer without calcium and loaded with 5μM Fura-2 acetoxymethylester (Invitrogen) in the presence of 0.2 μg/mL Pluronic F-127 (Biotium) at 37°C for 30 minutes. Loaded platelets, washed once and resuspended in Tyrode buffer containing 0.5mM EGTA (Roth) or 1mM Ca^{2+}, were activated with agonists. Calcium responses were measured under stirring with a spectrofluorimeter (LS 55, PerkinElmer), at alternate excitation wavelength of 340 and 380 nm (37°C). The 340/380 nm ratio values were converted into nanomolar concentrations of $[Ca^{2+}]$ by lysis with Triton X-100 (Sigma-Aldrich) and a surplus of

EGTA. Harvested MEG-01 cells were centrifuged at 530g for 5 minutes and then resuspended in RPMI medium (Invitrogen) and stained as described above. Measurements were performed in Ca^{2+} free Tyrode buffer. After incubation with 5μM thapsigargin (Invitrogen) for 10 minutes, 1mM Ca^{2+} was added. Isolated human platelets were incubated 60 minutes before measurement with the SGK1 inhibitor GSK650394 (1μM; Solvay), the SOCE inhibitor 2-APB (50μM; Sigma-Aldrich) or DMSO as solvent control at 37°C.

Western blot analysis

MEG-01 or HEK293 cells, freshly isolated human platelets, or pooled mouse platelets were centrifuged for 5 minutes at 240g, and the pellet was resuspended in lysis buffer (50mM Tris-HCl, pH 7.4, 150mM NaCl, 1% Trion-X, 0.5% Na_2HPO_4, 0.4% β-mercaptoethanol) containing protease inhibitor cocktail (Sigma-Aldrich). After centrifugation for 30 minutes at 20 000g and 4°C, the supernatant was taken and the protein concentration was measured with Bradford (Bio-Rad). For immunoblotting, proteins were electrotransferred onto a nitrocellulose membrane and blocked with 5% nonfat milk or 5% BSA at room temperature for 1 hour. Then, the membrane was incubated with the primary antibody against SGK1 (1:100; Pineda), Orai1 (1 μg/mL; Abcam), phospho-IKKα/β (Ser176/180; 1:1000, Cell Signaling), or phospho-IκBα (Ser32/36 1:1000; Cell Signaling) at 4°C overnight. After washing with TBST, the blots were incubated with secondary antibody conjugated with HRP (1:2000; Cell Signaling) for 1 hour at room temperature. After washing, antibody binding was detected with the ECL detection reagent (GE Healthcare). Bands were quantified with Quantity One Software (Bio-Rad). Membrane protein extraction was performed as described in supplemental Methods.

Immunofluorescence and confocal microscopy

Washed platelets were allowed to adhere to a fibrinogen surface (20 μg/mL) on a chamber slide; MEG-01 cells and murine megakaryocytes were adhered to poly-L-lysine (Sigma-Aldrich). Adherent platelets, megakaryocytes, and MEG-01 or HEK293 cells were fixed with paraformaldehyde (2%), washed and blocked with 2% BSA for 30 minutes, followed by incubation with the primary antibody for 2 hours at room temperature. Primary antibodies against SGK1 (1:100; Pineda), Orai1 (1:1000; Millipore), NF-κB p65 (1:250; Santa Cruz Biotechnology), and GP1bα (1:200; Emfret) were used. Chamber slides were washed and incubated with a FITC- or Cy3-conjugated secondary antibody (Santa Cruz Biotechnology). The actin cytoskeleton was stained with rhodamine-phalloidin (Invitrogen); nuclei were stained with DRAQ-5 dye (1:2000; Biostatus). The slides were mounted with ProLong Gold antifade reagent (Invitrogen). Confocal microscopy was performed using a Zeiss LSM5 EXCITER Confocal Laser Scanning Microscope (Carl Zeiss Micro Imaging) with a A-Plan 63× ocular.

Flow chamber

Heparinized whole mouse blood was diluted 1:3 in modified Tyrode buffer and perfused through a transparent flow chamber (slit depth, 50 μm) over a collagen-coated surface (200 μg/mL) with a wall shear rate of $1700s^{-1}$ for 5 minutes. After perfusion, the chamber was rinsed for 5 minutes by perfusion with Tyrode buffer, and pictures were taken from 5 or 6 different microscopic areas (×20, Carl Zeiss). Analysis was done with AxioVision (Carl Zeiss), and the mean percentage value of the covered area was determined.

Bleeding time

Mice were anesthetized, and a 3-mm segment of the tail tip was removed with a scalpel. Tail bleeding was monitored by gentle absorption of the blood with filter paper at 20-second intervals without making contact with the wound site. When no blood was observed on the paper, bleeding was determined to have ceased. Experiments were stopped after 20 minutes.

Statistical analysis

Data are given as mean ± SD or SEM; n represents the number of experiments. All data were tested for significance using paired or unpaired Student t test and 1-way ANOVA with Dunnet posthoc test.

Results

In an initial experiment, expression of the SGK1 was analyzed in human as well as in murine platelets and megakaryocytes. RT-PCR analysis, confocal microscopy, and Western blot analysis of human platelets revealed strong expression of SGK1 in platelets both at mRNA and protein levels (Figure 1A-B). The expression level was comparable with that in HEK293 cells.

To study the functional role of SGK1 in regulating platelet function, platelets and megakaryocytes were isolated from mice lacking SGK1 ($sgk1^{-/-}$) and respective wild-type littermates ($sgk1^{+/+}$). RT-PCR analysis, immunofluorescence staining, and Western blotting confirmed the absence of sgk1 mRNA and SGK1 protein in $sgk1^{-/-}$ platelets (Figure 1C-D) and megakaryocytes (Figure 1E-F).

$Sgk1^{-/-}$ mice appeared healthy and did not exhibit spontaneous bleeding. Blood platelet counts and mean platelet volume were similar in $sgk1^{+/+}$ and $sgk1^{-/-}$ mice (Table 1), indicating that SGK1 is not essential for platelet generation. In addition, no differences were found in other hematologic parameters (Table 1) or platelet-specific glycoproteins (supplemental Figure 1).

To elucidate the impact of SGK1 on platelet activation, platelet degranulation, integrin $\alpha_{IIb}\beta_3$ activation, and phosphatidylserine exposure flow cytometric measurements were performed. Degranulation-dependent P-selectin surface exposure was quantified before and after activation with ADP (10μM), thrombin (0.02 U/mL) as well as the specific agonists of the collagen receptor GPVI, CVX (1 μg/mL), and CRP (5 μg/mL). As illustrated in Figure 2A, P-selectin abundance at the platelet surface was significantly lower in $sgk1^{-/-}$ platelets than in $sgk1^{+/+}$ platelets after stimulation with CVX and CRP. Degranulation after stimulation with thrombin tended to be lower in $sgk1^{-/-}$ platelets than in $sgk1^{+/+}$ platelets, a difference, however, not reaching statistical significance.

After stimulation with CVX and CRP, surface expression of activated integrin $\alpha_{IIb}\beta_3$ was significantly lower in $sgk1^{-/-}$ platelets than in $sgk1^{+/+}$ platelets (Figure 2B). After low-dose concentrations of thrombin or ADP, the activation of integrin $\alpha_{IIb}\beta_3$ was not significantly different between $sgk1^{-/-}$ and $sgk1^{+/+}$ platelets.

For examination of activation-dependent phosphatidylserine exposure, platelets were stimulated with thrombin (1.0 U/mL), CVX (1 μg/mL), or thrombin/CVX (0.05 U/mL/0.5 μg/mL) and annexin-positive cells were analyzed by flow cytometry. After stimulation with thrombin, CVX or the combination (thrombin/CVX), surface exposure of phosphatidylserine was significantly lower in $sgk1^{-/-}$ platelets than in $sgk1^{+/+}$ platelets (Figure 2C).

To determine whether impaired degranulation, integrin $\alpha_{IIb}\beta_3$ activation, and phosphatidylserine exposure would translate into functional deficits in $sgk1^{-/-}$ platelets, we performed impedance measurements of platelet aggregation before and after activation with low or high concentrations of CRP (1 and 10 μg/mL), collagen (1 and 5 μg/mL), PAR-4 activating peptide (125 and 500μM), and ADP (2.5 and 10μM). As illustrated in Figure 2D, platelet aggregation after stimulation with low-dose concentrations of the GPVI-acting ligands collagen or CRP was significantly less pronounced in $sgk1^{-/-}$ platelets than in $sgk1^{+/+}$ platelets. Only a slight difference was found after stimulation with low-dose PAR-4
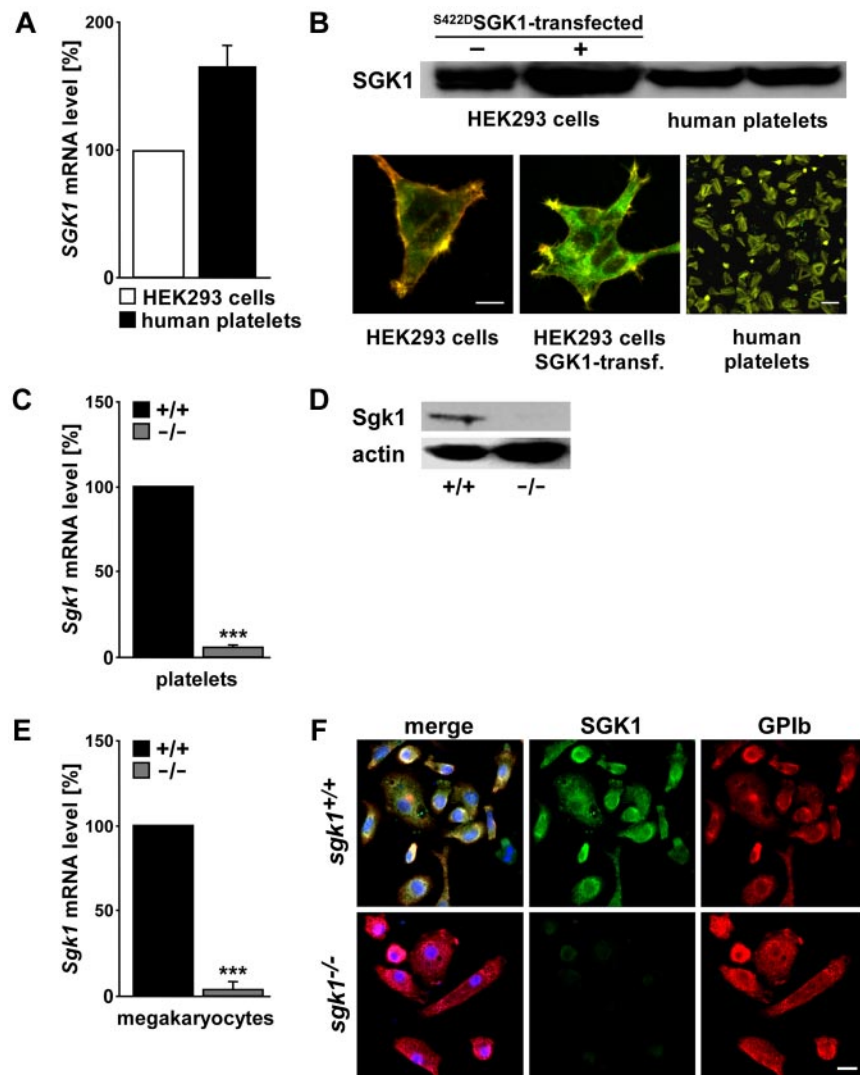
Figure 1. SGK1 mRNA and protein expression in human as well as in murine platelets and megakaryocytes. (A) Quantitative RT-PCR of mRNA encoding SGK1 in human platelets and HEK293 cells. (B) Western blot and confocal microscopy of SGK1 abundance in human platelets, nontransfected and ^{S422D}SGK1-transfected HEK293 cells. Red represents actin; and green, SGK1. Bar represents 5 μm. (C) Arithmetic mean ± SEM (n = 4) of mRNA encoding SGK1 in platelets from $sgk1^{-/-}$ mice expressed in percentage of the respective value in platelets from $sgk1^{+/+}$ mice. ***$P < .001$. (D) Representative Western blot analysis of SGK1 protein abundance in platelets from $sgk1^{+/+}$ and $sgk1^{-/-}$ mice. (E) Arithmetic mean ± SEM (n = 4) of mRNA encoding SGK1 in megakaryocytes from $sgk1^{-/-}$ mice expressed in percentage of the respective value in megakaryocytes from $sgk1^{+/+}$ mice. ***$P < .001$. (F) Confocal microscopy of SGK1 protein abundance in megakaryocytes from $sgk1^{+/+}$ (top) and $sgk1^{-/-}$ (bottom) mice. Red represents glycoprotein Ib; green, SGK1; and blue, nuclei. Bar represents 10 μm.

activating peptide, an agonist of the principal murine thrombin receptor. The aggregation defect found in $sgk1^{-/-}$ platelets was overcome by increasing the agonist concentration.

To elucidate the relevance of SGK1 in pathologic thrombus formation, we examined platelet adhesion to collagen-coated surfaces under flow at high arterial shear rates ($1700s^{-1}$). As illustrated in Figure 2E, $sgk1^{+/+}$ platelets formed massive and dense thrombi after 5 minutes of perfusion, whereas $sgk1^{-/-}$ platelets formed only some smaller single thrombi with a significantly reduced thrombus surface coverage. To test whether the defect in $sgk1^{-/-}$ platelets impaired hemostasis, we measured tail bleeding time. As shown in Figure 2F, the bleeding time was not significantly different in $sgk1^{-/-}$ mice compared with $sgk1^{+/+}$ mice.

Platelet activation, including integrin $\alpha_{IIb}\beta_3$ activation, granule release, phosphatidylserine exposure, aggregation, and thrombus formation, are directly dependent on an increase in the intracellular Ca^{2+} concentration ($[Ca^{2+}]_i$). Spectrofluorimetric measurements were thus used to elucidate the impact of SGK1 on the increase of cytosolic Ca^{2+} activity after platelet activation by thrombin (0.02 U/mL), CVX (1 μg/mL), CRP (10 μg/mL), and ADP (10μM).

To discriminate between intracellular Ca^{2+} store release and Ca^{2+} influx from extracellular space, we performed measurements of activation-dependent changes in $[Ca^{2+}]_i$ in the presence (1mM Ca^{2+}) and absence (0.5mM EGTA) of extracellular Ca^{2+} (Figure 3A-B). Before stimulation, the cytosolic Ca^{2+} concentration was similar in $sgk1^{+/+}$ and $sgk1^{-/-}$ platelets. In the presence of extracellular Ca^{2+} all agonists triggered an increase of cytosolic Ca^{2+} activity in $sgk1^{+/+}$ and $sgk1^{-/-}$ platelets. The increase of cytosolic Ca^{2+} activity was, however, less pronounced in $sgk1^{-/-}$ platelets than in $sgk1^{+/+}$ platelets, a difference reaching statistical significance after stimulation with CVX and CRP (Figure 3A-B). In the absence of extracellular Ca^{2+}, the increase of cytosolic Ca^{2+} activity after stimulation with either agonist was similar in $sgk1^{-/-}$ and $sgk1^{+/+}$ platelets.

The impaired agonist induced Ca^{2+} response in the presence of extracellular Ca^{2+} pointed to an impaired SOCE in SGK1-deficient platelets. To test this hypothesis, SOCE was induced in $sgk1^{+/+}$ and $sgk1^{-/-}$ platelets with saroplasmatic reticulum (SR) Ca^{2+} ATPase

Table 1. Blood count of $sgk1^{+/+}$ and $sgk1^{-/-}$ mice

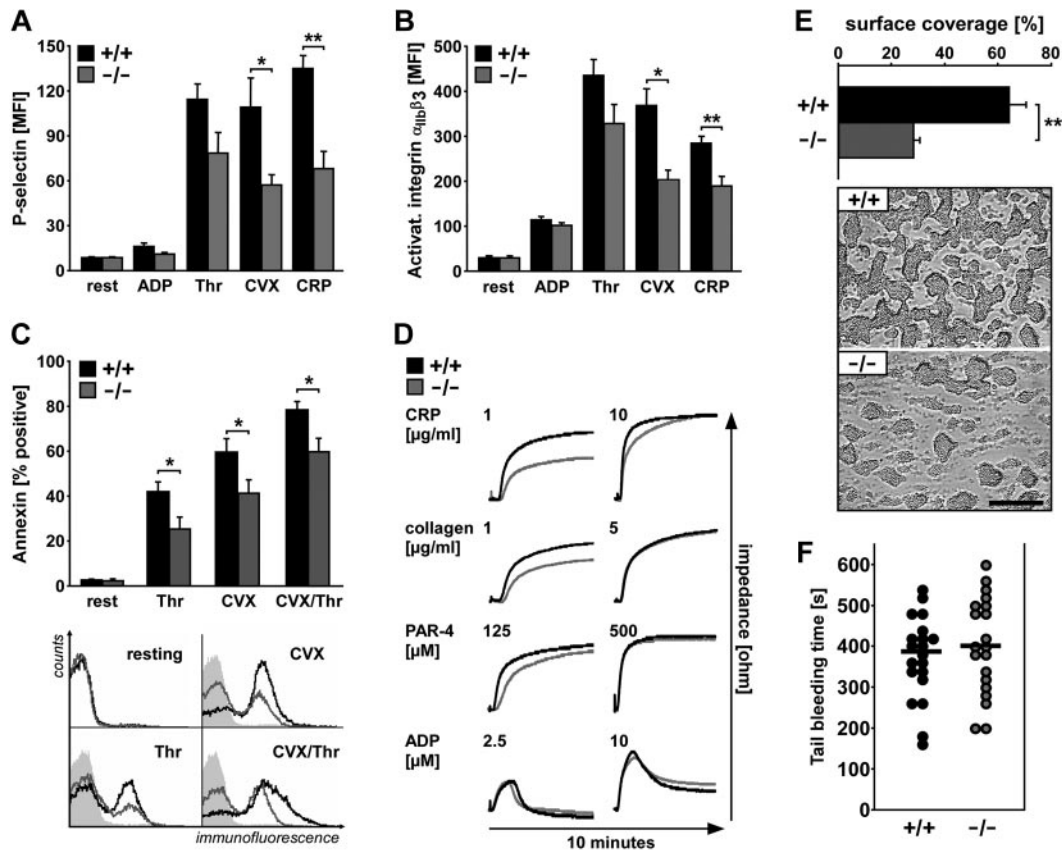|	$sgk1^{+/+}$	$sgk1^{-/-}$
Platelets, $\times 10^3/\mu L$	1023 ± 175	1020 ± 99
Mean platelet volume, fL	6.4 ± 0.2	6.5 ± 0.3
Erythrocytes, $\times 10^6/\mu L$	9.7 ± 1.2	9.7 ± 1.2
Hemoglobin, g/dL	14.3 ± 1.3	14.0 ± 1.0
Hematocrit, %	41.4 ± 3.9	40.6 ± 2.9
Mean corpuscular volume, fL	42.7 ± 2.2	42.0 ± 1.6

Figure 2. Activation-dependent platelet degranulation, $\alpha_{IIb}\beta_3$integrin activation, phosphatidylserine exposure, and aggregation as well as in vitro thrombus formation and tail bleeding time. (A) Flow cytometric analysis of degranulation-dependent P-selectin exposure in platelets from $sgk1^{+/+}$ (black bar) and $sgk1^{-/-}$ (gray bar) mice in response to 10 μM ADP, 0.02 U/mL thrombin, 1 μg/mL CVX, and 5 μg/mL CRP. Arithmetic mean ± SEM (n = 6). *$P < .05$. **$P < .01$. (B) Flow cytometric analysis of $\alpha_{IIb}\beta_3$ integrin activation in platelets from $sgk1^{+/+}$ (black bar) and $sgk1^{-/-}$ (gray bar) mice in response to 10 μM ADP, 0.02 U/mL thrombin, 1 μg/mL CVX, and 5 μg/mL CRP. Arithmetic mean ± SEM (n = 6). *$P < .05$. **$P < .01$. (C) Flow cytometric analysis of phosphatidylserine exposure in platelets from $sgk1^{+/+}$ (black bar) and $sgk1^{-/-}$ (gray bar) mice in response to 1.0 U/mL thrombin, 1 μg/mL CVX, and 0.05 U/mL thrombin + 0.5 μg/mL CVX. (Top) Arithmetic mean ± SEM (n = 9). *$P < .05$. (Bottom) Representative overlays of annexin-positive $sgk1^{+/+}$ (black line) and $sgk1^{-/-}$ (gray line) platelets. Light gray panels represent isotype controls. (D) Impedance aggregometry after stimulation with different concentrations of CRP (1 and 10 μg/mL), collagen (1 and 5 μg/mL), PAR-4 activating peptide (125 and 500 μM), and ADP (2.5 and 10 μM). Representative aggregation tracings of $sgk1^{+/+}$ (black line) and $sgk1^{-/-}$ (gray line) mice (n = 4). (E) Thrombus formation in vitro. Whole blood from $sgk1^{+/+}$ and $sgk1^{-/-}$ mice was perfused over a collagen-coated surface for 5 minutes at a shear rate of $1700s^{-1}$. Arithmetic mean ± SEM (n = 6; top) and representative phase-contrast images (bottom) of surface coverage. **$P < .01$. Bar represents 50 μm. (F) Tail bleeding time measured after amputating the tail tip of $sgk1^{+/+}$ and $sgk1^{-/-}$ mice. Each dot represents 1 mouse; black bar represents the mean value.

pump inhibitor thapsigargin. In the absence of extracellular Ca^{2+}, thapsigargin (5 μM) triggered a Ca^{2+} release from intracellular stores (store release) that was similar in $sgk1^{+/+}$ platelets and in $sgk1^{-/-}$ platelets (Figure 3C). The subsequent addition of extracellular Ca^{2+} in the continued presence of thapsigargin triggered an SOCE, which was significantly less pronounced in $sgk1^{-/-}$ platelets than in $sgk1^{+/+}$ platelets. These results demonstrate, for the first time, that SGK1 is a regulator of platelet SOCE contributing to the regulation of cytosolic Ca^{2+} activity in platelets and platelet activation.

To test whether the decreased SOCE in sgk1$^{-/-}$ could have been the result of a decreased cell membrane protein abundance of the major platelet SOCE-mediating channel Orai1, we compared the Orai1 protein expression in $sgk1^{+/+}$ and $sgk1^{-/-}$ platelets. As shown in Figure 4A-D, Western blotting, immunofluorescence/confocal microscopy, and FACS analysis all disclosed that Orai1 protein (membrane) abundance was significantly lower in $sgk1^{-/-}$ platelets than in $sgk1^{+/+}$ platelets, whereas STIM1 expression was not significantly different.

Immunofluorescence/confocal microscopy revealed that Orai1 protein abundance was again significantly lower in $sgk1^{-/-}$ megakaryocytes compared with $sgk1^{+/+}$ megakaryocytes (Figure 4E).

Further experiments were performed in the human megakaryocytic cell line MEG-01, an extensively used model of human megakaryocytes.[28] According to confocal microscopy and Western blot analysis, the protein abundance of Orai1 in the plasma membrane of MEG-01 cells was significantly increased after transfection with the constitutively active mutant ^{S422D}SGK1 but not after transfection with the inactive mutant ^{K127N}SGK1 (Figure 5A-B). Addition of the store-depleting SR/endoplasmic reticulum Ca^{2+} ATPase inhibitor thapsigargin (5 μM) in nominally Ca^{2+}-free solution was followed by rapid, transient increase in cytosolic Ca^{2+} in MEG-01 cells (Figure 5C). Subsequent addition of Ca^{2+} to the extracellular medium resulted in a rapid and sustained increase in cytosolic Ca^{2+} because of SOCE. Both slope and peak of MEG-01 SOCE were significantly enhanced by transient expression of the constitutively active mutant ^{S422D}SGK1 but not of the inactive mutant ^{K127N}SGK1 (Figure 5C).

The basal Fura-2 fluorescence ratio, reflecting resting intracellular Ca^{2+} concentration, was similar in MEG-01 cells transfected with control plasmid, in MEG-01 cells transfected with ^{S422D}SGK1 and in MEG-01 cells transfected with ^{K127N}SGK1. Moreover, the Ca^{2+} release from intracellular stores after thapsigargin (5 μM) treatment was not significantly different between MEG-01 cells
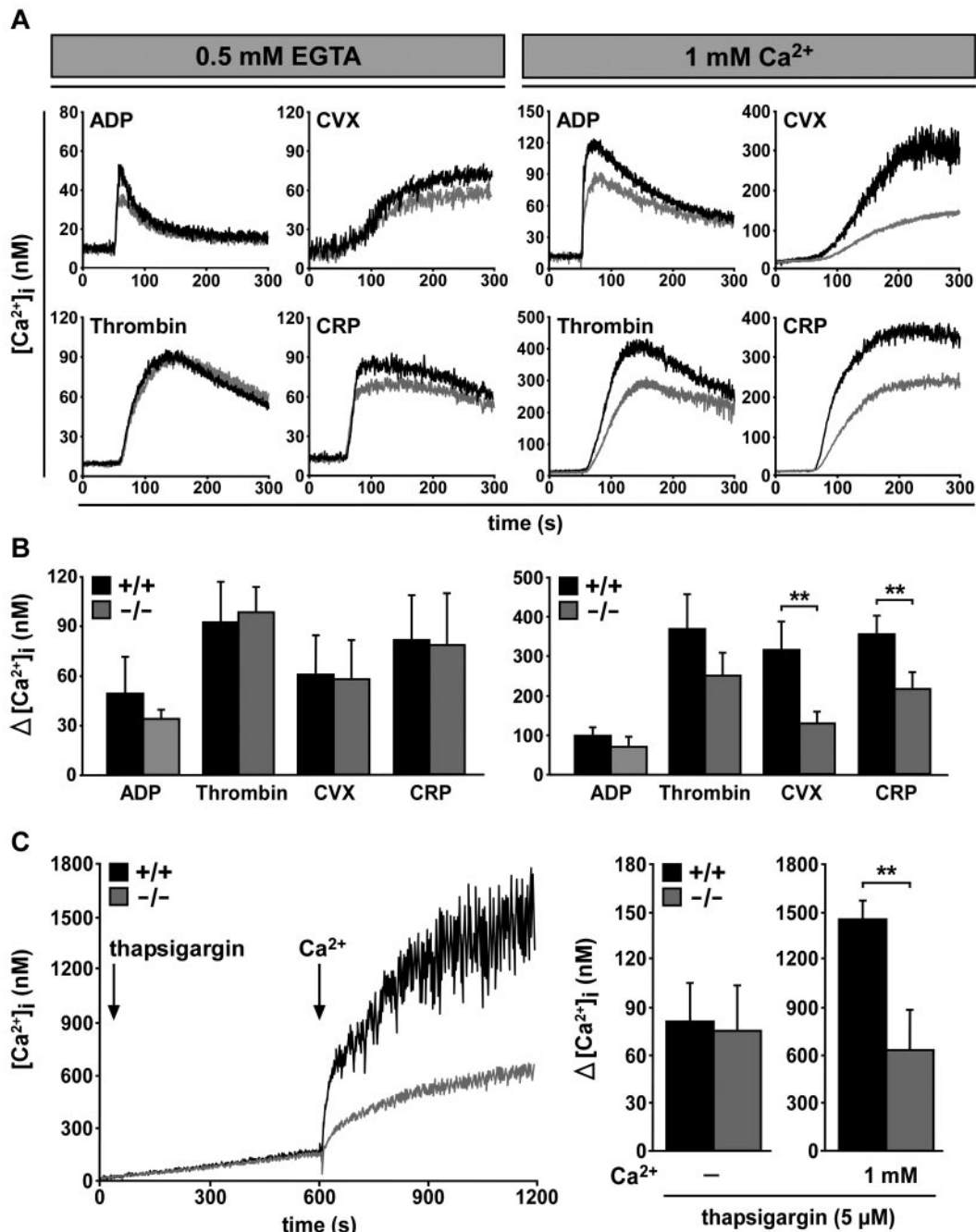
Figure 3. Agonist-induced Ca²⁺ response and impaired SOCE in *sgk1⁻/⁻* and *sgk1⁺/⁺* platelets. (A) Representative tracings of Fura-2-fluorescence reflecting cytosolic Ca²⁺ concentration [Ca²⁺]ᵢ of *sgk1⁺/⁺* (black line) and *sgk1⁻/⁻* (gray line) platelets before and after stimulation with thrombin (0.02 U/mL), CVX (1 µg/mL), CRP (10 µg/mL), and ADP (10µM) in the absence (0.5mM EGTA, left) or presence (1mM Ca²⁺, right) of extracellular Ca²⁺. (B) Arithmetic mean of maximal Δ[Ca²⁺]ᵢ ± SD (n = 4 per group). **P < .01. (C) Fura-2-fluorescence reflecting cytosolic Ca²⁺ concentration [Ca²⁺]ᵢ of *sgk1⁺/⁺* (black line) and *sgk1⁻/⁻* (gray line) platelets after exposure to 5µM thapsigargin in the nominal absence of extracellular Ca²⁺ for 10 minutes and subsequent addition of 1mM extracellular Ca²⁺. Representative tracings (left) and arithmetic mean (right) of maximal Δ[Ca²⁺]ᵢ ± SD (n = 6 per group) before and after addition of 1mM Ca²⁺. **P < .01.

transfected with control plasmid, MEG-01 cells transfected with ^S422D^SGK1, and MEG-01 cells transfected with ^K127N^SGK1 (Figure 5C). The specific SGK1 inhibitor GSK650394 (1µM) abolished the ^S422D^SGK1-induced up-regulation of Orai1 expression and SOCE (Figure 5D-E).

Quantitative RT-PCR revealed that Orai1 mRNA levels were significantly lower in *sgk1⁻/⁻* platelets and megakaryocytes than in *sgk1⁺/⁺* platelets and megakaryocytes (Figure 6A). Transfection of MEG-01 cells with ^S422D^SGK1, but not with ^K127N^SGK1, significantly increased Orai1 mRNA levels (Figure 6B). Those observa-

tions pointed to SGK1-sensitive transcriptional regulation of Orai1 in megakaryocytes.

Further experiments aimed to disclose the underlying mechanism of SGK1-dependent transcriptional regulation of Orai1. Transfection with ^S422D^SGK1, but not transfection with ^K127N^SGK1, significantly increased phosphorylation of the NF-κB regulating kinases IKKα/β (Figure 6C) and IκBα (Figure 6D) in MEG-01 cells. The up-regulation of Orai1 mRNA 48 hours after ^S422D^SGK1 transfection was abrogated after a 24-hour incubation with the highly selective IKK inhibitor BMS-345541 (10µM) or the SGK1
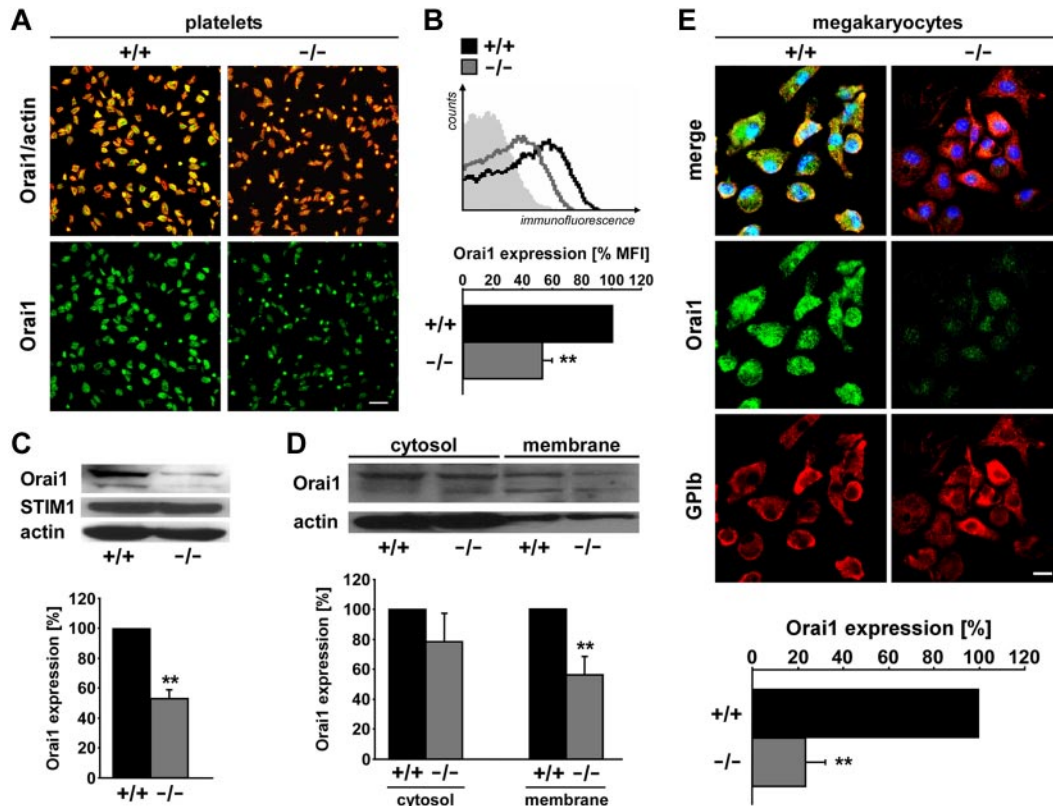
Figure 4. Orai1 protein abundance in *sgk1^{−/−}* and *sgk1^{+/+}* platelets and megakaryocytes. (A) Confocal microscopy of Orai1 protein abundance in platelets from *sgk1^{+/+}* (left panels) and *sgk1^{−/−}* (right panels) mice. Red represents actin; and green, Orai1. Bar represents 10 μm. (B) Flow cytometric analysis of Orai1 surface expression in platelets from *sgk1^{+/+}* (black bar) and *sgk1^{−/−}* (gray bar) mice. (Bottom) Arithmetic mean ± SEM (n = 7). **$P < .01$. (Top) Representative overlays of Orai1-positive *sgk1^{+/+}* (black line) and *sgk1^{−/−}* (gray line) platelets; light gray panel represents isotype control. (C) Western blot analysis of whole cell lysate protein of Orai1 and STIM1 from *sgk1^{+/+}* and *sgk1^{−/−}* platelets. Arithmetic mean ± SEM (n = 4) of Orai1 protein abundance in *sgk1^{+/+}* (black bar) and *sgk1^{−/−}* (gray bar) platelets. **$P < .01$. (D) Western blot analysis of isolated membrane protein and cytosolic fraction of Orai1 from *sgk1^{+/+}* and *sgk1^{−/−}* platelets. Arithmetic mean ± SEM (n = 4) of Orai1 protein abundance in *sgk1^{+/+}* (black bars) and *sgk1^{−/−}* (gray bars) platelets. **$P < .01$. (E) Confocal microscopy of Orai1 protein abundance in megakaryocytes cultivated from bone marrow of *sgk1^{+/+}* (left panels) and *sgk1^{−/−}* (right panels) mice (top). Red represents GPIb; green, Orai1; and blue, nuclei. Bar represents 10 μm. Statistical analysis of Orai1 immunofluorescence abundance (bottom). **$P < .01$. n = 4.

inhibitor GSK650394 (1μM; Figure 6E). Furthermore, the [S422D]SGK1-induced up-regulation of SOCE could be inhibited by treatment with BMS-345541 (10μM; Figure 6F). Finally, as evident from immunofluorescence/confocal microscopy, the nuclear translocation of the NF-κB subunit p65 reflecting transcriptional activity was significantly less pronounced in *sgk1^{−/−}* megakaryocytes than in *sgk1^{+/+}* megakaryocytes (Figure 6G). Consistent with that finding, we found an increased expression of p65 in isolated nuclear fractions of MEG-01 cells transfected with [S422D]SGK1 compared with untransfected MEG-01 cells or to cells transfected with [K127N]SGK1 (supplemental Figure 5).

Discussion

Platelets play a central role in the pathogenesis of arterial thrombosis and the mechanisms regulating the adhesive functions of platelets are thus of pivotal importance for occlusive cardiovascular disease.[1,23] The present study unravels a novel regulator of platelet function, the PI3K pathway downstream effector SGK1. SGK1 belongs to the AGC family of serine-threonine kinases and shares a relatively high degree of homology with Akt in its catalytic domain.[16,17] Previous work has identified a critical role for PI3K[13-15] and some of its downstream effectors (eg, the AGC family members Akt[12,29] and protein kinase C[30]) in promoting and maintaining platelet activation, including activation-dependent

Ca^{2+} signaling. But the molecular targets of the products of PI3K in their respective functions have been incompletely defined.[29] In this study, we could show, for the first time, that SGK1 is a novel important regulator of cytosolic Ca^{2+} and function of platelets and megakaryocytes.

Similar to observations in platelets completely lacking Orai1[7] or expressing a functional inactive Orai1 mutant ([R93W]Orai1),[6] the impact of SGK1 deficiency on activation-dependent degranulation or integrin $\alpha_{IIb}\beta_3$ activation is more pronounced after application of GPVI agonists than after administration of thrombin or ADP. Possibly, thrombin or ADP stimulates in addition Orai1 independent Ca^{2+} entry, whereas Orai1-mediated Ca^{2+} entry is particularly important for GPVI-ITAM-mediated cell activation.[31]

The decreased activation of integrin $\alpha_{IIb}\beta_3$ in platelets lacking SGK1 paralleled a deficit in the ability of these platelets to undergo aggregation at low-dose concentrations of agonists. Increasing the agonists concentrations dissipated the differences between *sgk1^{−/−}* and *sgk1^{+/+}* platelets, indicating that SGK1 deficiency enhances the sensitivity of platelets to activating agonists but does not modify the maximal effect after full activation. Apparently, the abundance of Orai1 is limiting after moderate but not after full platelet activation. Clearly, SGK1 deficiency does not abrogate SOCE and Ca^{2+}-sensitive platelet function but decreases the sensitivity of the platelets to stimulators of Ca^{2+} entry. In the absence of SGK1, apparently other signaling molecules, such as Akt, maintain basic platelet function. Thus, in contrast to the severe
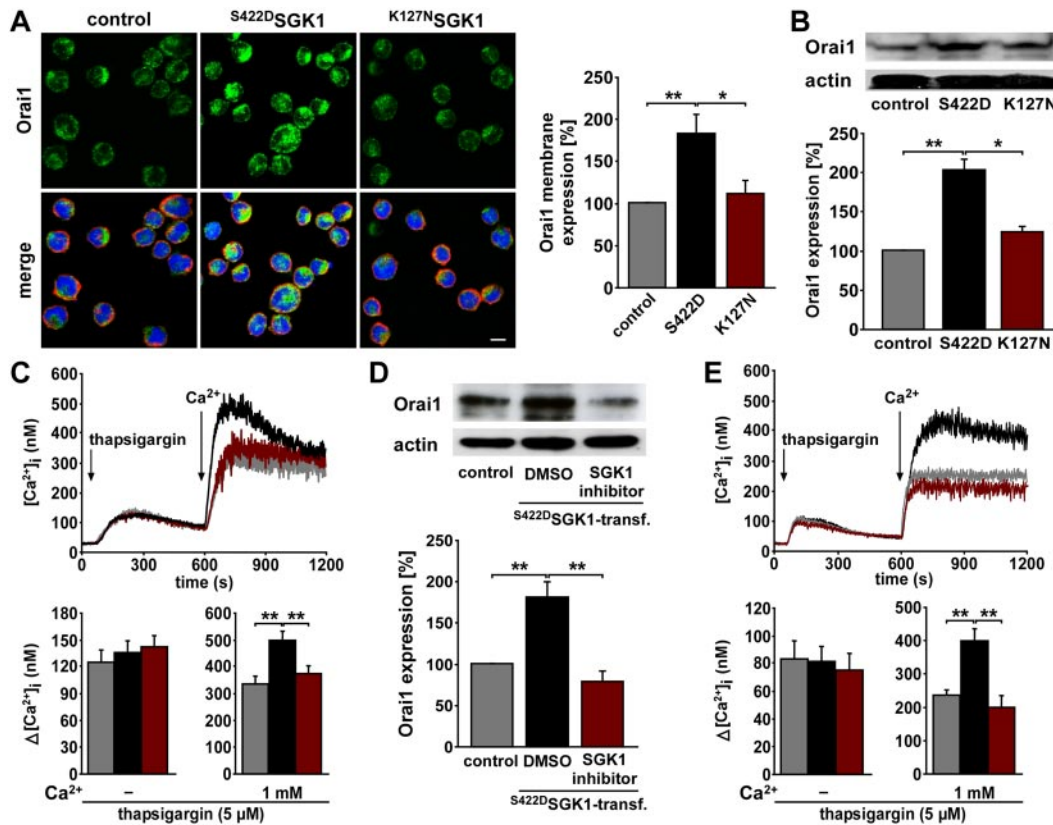
Figure 5. SGK1-dependent Orai1 membrane abundance and SOCE in megakaryocytic cell line MEG-01. (A) Confocal microscopy of Orai1 membrane abundance in nontransfected (control plasmid), ^{S422D}SGK1-transfected, and ^{K127N}SGK1-transfected MEG-01 cells (left). Red represents actin; green, Orai1; and blue, nuclei. Scale bar represents 10 μm. Statistical analysis of Orai1 immunofluorescence membrane abundance (right). $^*P < .05$. $^{**}P < .01$. n = 4. (B) Western blot analysis of Orai1 membrane abundance in nontransfected (control plasmid), ^{S422D}SGK1-transfected, and ^{K127N}SGK1-transfected MEG-01 cells. Arithmetic mean ± SEM (n = 7) of Orai1 protein abundance. $^*P < .05$. $^{**}P < .01$. (C) SOCE in SGK1-transfected MEG-01 cells. Fura-2-fluorescence reflecting cytosolic Ca^{2+} concentration [Ca^{2+}]$_i$ of MEG-01 cells transfected with control-plasmid (gray), ^{S422D}SGK1 (black), or ^{K127N}SGK1 (red) after exposure to 5μM thapsigargin (Ca^{2+} store depletion) in the nominal absence of extracellular Ca^{2+} for 10 minutes and subsequent addition of 1mM extracellular Ca^{2+}. Representative tracings (top) and arithmetic mean (bottom) of maximal Δ[Ca^{2+}]$_i$ ± SEM (n = 15 per group) before and after addition of 1mM Ca^{2+}. $^{**}P < .01$. (D) Western blot analysis of Orai1 membrane abundance in nontransfected (control plasmid) MEG-01 cells and in ^{S422D}SGK1-transfected MEG-01 cells treated with the SGK1 inhibitor GSK650394 (1μM) or DMSO as solvent control. Arithmetic mean ± SEM (n = 4) of Orai1 protein abundance. $^{**}P < .01$. (E) SOCE in MEG-01 cells treated with the specific SGK1 inhibitor GSK650394. Fura-2 fluorescence reflecting cytosolic Ca^{2+} concentration [Ca^{2+}]$_i$ of MEG-01 cells transfected with control plasmid (gray) or ^{S422D}SGK1-transfected MEG-01 cells after treatment with GSK650394 (1μM, red) or DMSO (black) as solvent control. Representative tracings (top) and arithmetic mean (bottom) of maximal Δ[Ca^{2+}]$_i$ ± SEM (n = 9 per group) after exposure to 5μM thapsigargin (Ca^{2+} store depletion) in the nominal absence of extracellular Ca^{2+} for 10 minutes and subsequent addition of 1mM extracellular Ca^{2+}. $^{**}P < .01$.

phenotype of Orai1-deficient mice,[7] the phenotype of $sgk1^{-/-}$ mice is mild.

Rupture of an atherosclerotic lesion leads to endothelial denudation and exposure of the thrombogenic subendothelial collagen to circulating platelets, initiating platelet recruitment to the injured vessel wall.[32] According to the present study, lack of SGK1 decreases collagen-triggered thrombus formation under high shear stress. Platelet responses, including degranulation, integrin $\alpha_{IIb}\beta_3$ activation, thrombus formation, and especially phosphatidylserine exposure, which collectively accomplish platelet procoagulant activity, critically depend on an increase in [Ca^{2+}]$_i$.[3,33] An increase of [Ca^{2+}]$_i$ may result from release of intracellular Ca^{2+} compartmentalized in endoplasmic reticulum and entry of extracellular Ca^{2+} triggered by the depletion of SR Ca^{2+} stores, the SOCE.[2]

SGK1 deficiency markedly decreased platelet SOCE. Although the filling and release of the intracellular Ca^{2+} stores were unaffected in $sgk1^{-/-}$ platelets, SOCE was markedly reduced in platelets of SGK1-deficient mice. Furthermore, $sgk1^{-/-}$ platelets and megakaryocytes expressed less Orai1 Ca^{2+} channel protein in their cell membrane. Orai1 is a plasma membrane protein and the pore-forming unit for the SOCE.[34] Orai1 is regulated by STIM1.[35] STIM1 senses the Ca^{2+} content of the intracellular stores in platelet

endoplasmic reticulum (dense tubular system) and activates the plasma membrane Orai1 on store depletion.[8] Both Orai1 and STIM1 have previously been shown to be critically important for proper function of platelets.[7,8] Besides the decreased Orai1 protein abundance in $sgk1^{-/-}$ platelets, SGK1 sensitivity of Orai1 expression was apparent from transfections with the constitutively active mutant (^{S422D}SGK1) or the inactive mutant (^{K127N}SGK1) of SGK1 in the human megakaryoblastic cell line MEG-01, cells with many properties in common with normal human megakaryocytes at an early stage of maturation.[36] MEG-01 cells regulate the cytosolic Ca^{2+} concentration in response to activation or store depletion via the same mechanisms, which are operative in platelets and megakaryocytes.[37] Furthermore, MEG-01 cells highly express the store-operated Ca^{2+} channel Orai1 as well as the store Ca^{2+} sensor STIM1[38] and thus represent an ideal model for studying mechanisms regulating SOCE in human megakaryocytes. Transfection with the constitutively active mutant ^{S422D}SGK1, but not transfection with the inactive mutant ^{K127N}SGK1, significantly increased Orai1 membrane abundance and SOCE, an effect abrogated in the presence of GSK650394 (1μM), a specific SGK1 inhibitor.[39] Accordingly, SGK1 regulates membrane expression of Orai1 and SOCE in megakaryocytes.
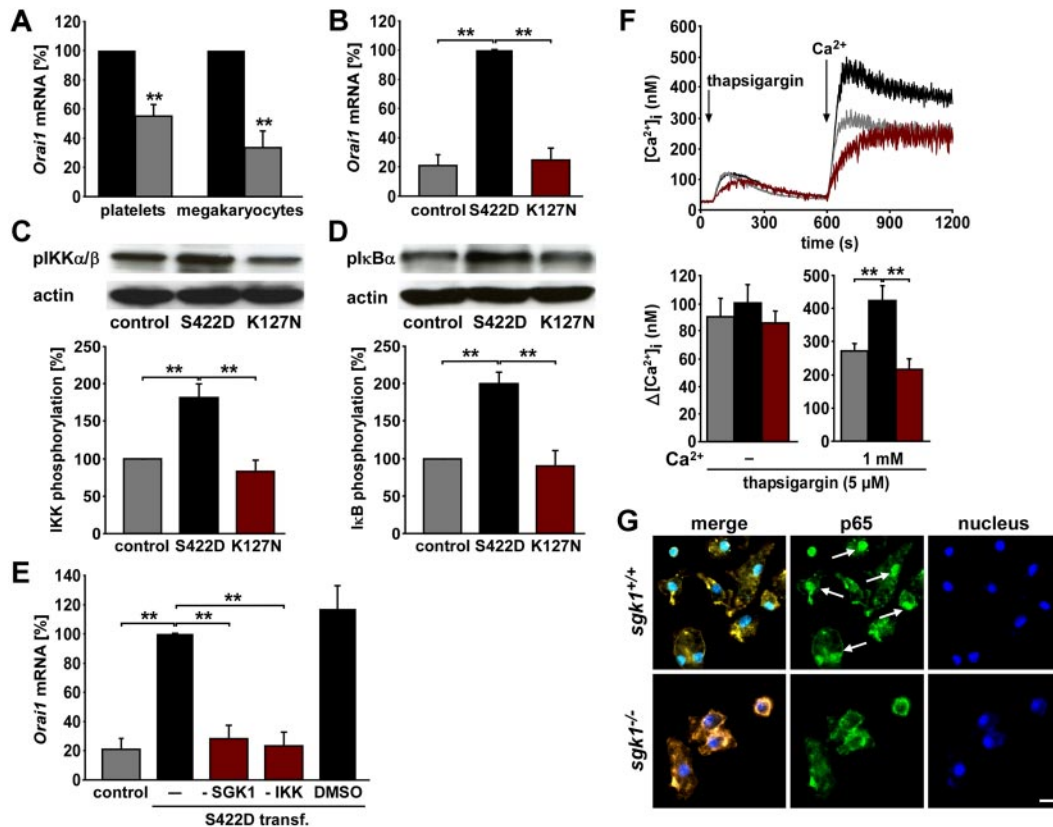
Figure 6. SGK1-sensitive NF-κB–dependent transcription in MEG-01 cells und primary megakaryocytes. (A) Arithmetic mean ± SEM (n = 4) of mRNA encoding Orai1 in platelets (left) and megakaryocytes (right) from $sgk1^{+/+}$ (black bar) and $sgk1^{-/-}$ mice (gray bar). **$P < .01$. (B) Arithmetic mean ± SEM (n = 6) of mRNA encoding Orai1 in nontransfected (control plasmid), ^{S422D}SGK1-transfected, and ^{K127N}SGK1-transfected MEG-01 cells of Orai1 mRNA abundance. **$P < .01$. (C) Western blot analysis of phospho-IKKα/β in nontransfected (control plasmid), ^{S422D}SGK1-transfected, and ^{K127N}SGK1-transfected MEG-01 cells. Arithmetic mean ± SEM (n = 5) of IKKα/β phosphorylation. **$P < .01$. (D) Western blot analysis of phospho-IκBα in nontransfected (control plasmid), ^{S422D}SGK1-transfected, and ^{K127N}SGK1-transfected MEG-01 cells. Arithmetic mean ± SEM (n = 5) of IκBα phosphorylation. **$P < .01$. (E) Arithmetic mean ± SEM (n = 6) of mRNA encoding Orai1 in nontransfected (control plasmid) and ^{S422D}SGK1-transfected MEG-01 cells incubated with SGK1 inhibitor GSK650394 (1μM), IKK inhibitor BMS-345541 (10μM), or DMSO as solvent control. **$P < .01$. (F) SOCE in MEG-01 cells treated with the highly specific IKK inhibitor BMS-345541. Fura-2-fluorescence reflecting cytosolic Ca^{2+} concentration $[Ca^{2+}]_i$ of MEG-01 cells transfected with control-plasmid (gray), ^{S422D}SGK1-transfected MEG-01 cells treated with the IKK inhibitor BMS-345541 (10μM, red), or DMSO as solvent control (black) after exposure to 5μM thapsigargin (Ca^{2+} store depletion) in the nominal absence of extracellular Ca^{2+} for 10 minutes and subsequent addition of 1mM extracellular Ca^{2+}. Representative tracings (left) and arithmetic mean (right) of maximal $\Delta[Ca^{2+}]_i$ ± SEM (n = 8 per group) before and after addition of 1mM Ca^{2+}. **$P < .01$. (G) Confocal microscopy of nuclear translocation of the NF-κB subunit p65 (RelA) in murine megakaryocytes cultivated from bone marrow of $sgk1^{+/+}$ (top) and $sgk1^{-/-}$ (bottom) mice. Red represents GPIb; green, p65; and blue, nuclei. White arrows point to nuclear translocated p65. Bar represents 10 μm.

The decreased Orai1 protein abundance in $sgk1^{-/-}$ platelets could have resulted from decreased Orai1 transcription or accelerated degradation of Orai1 protein. As $sgk1^{-/-}$ platelets and megakaryocytes contain significantly less Orai1 mRNA than $sgk1^{+/+}$ platelets and megakaryocytes, SGK1 is at least partially effective by up-regulating Orai1 transcription. Similarly, Orai1 mRNA levels in MEG-01 cells were increased by transfection with ^{S422D}SGK1 but not by transfection with ^{K127N}SGK1. Apparently, SGK1 does not directly influence SOCE, agonist-induced Ca^{2+} entry, or Ca^{2+}-dependent platelet activation, as degranulation or integrin $\alpha_{IIb}\beta_3$ activation was not directly modified by SGK1 inhibitor GSK650394 (supplemental Figures 2 and 3).

Further experiments addressed the mechanism mediating SGK1-dependent Orai1 transcription. SGK1 is known to regulate transcription by up-regulating NF-κB activity through phosphorylation and activation of IKKα/β.[16,40] Thus, SGK1 enhances the ability of IKKα/β to phosphorylate endogenous IκBα.[41] The majority of NF-κB components, including the regulatory IκB and IKK, are expressed in both MEG-01 cells and human megakaryocytes.[42] Functionally, NF-κB has been shown to regulate megakaryocytic differentiation.[43] Thus, there is evolving evidence pointing to a decisive role of NF-κB in regulating gene expression in megakaryocytes. Nevertheless, megakaryocytic proteins, which are under transcriptional control of NF-κB and NF-κB–activating mechanisms in megakaryocytes, remain to be clarified. In the present study, transfection with ^{S422D}SGK1 but, not with ^{K127N}SGK1, significantly increased IKKα/β and IκBα phosphorylation in megakaryocytic MEG-01 cells. NF-κB activation could be disrupted by small-molecule inhibitors of IKKβ.[44] Accordingly, the highly selective IKK inhibitor BMS-345541 (10μM), which shows greater than 10-fold selectivity for IKKβ than for IKKα,[45] abrogated the up-regulation of Orai1 mRNA induced by transfection of MEG-01 cells with ^{S422D}SGK1 and abolished the SGK1-induced increase of SOCE (Figure 6F).

NF-κB is held latent in the cytoplasm as a complex bound with unphosphorylated IκB, thereby blocking the nuclear translocation of NF-κB.[46] Phosphorylation of IκB by IKK leads to proteosomal degradation of IκB, liberating the NF-κB dimers (mostly p50-p65 dimers) to translocate into the nucleus and initiate transcription of target genes.[47] Accordingly, nuclear translocation of p65 was less pronounced in $sgk1^{-/-}$ megakaryocytes than in $sgk1^{+/+}$ megakaryocytes, and transfection of MEG-01 cells with ^{S422D}SGK1 increased nuclear expression of p65.

IKKβ-dependent NF-κB activation plays a key role in inflammation and inflammatory signaling pathways in metabolic diseases[48] as diabetes or the metabolic syndrome, which are classically associated with platelet hyper-responsiveness and atherothrombotic complications, such as myocardial infarction or ischemic stroke.[49] Hyperglycemia, glucose-induced AGEs, and oxidative stress are powerful stimulators of SGK1[17] and its downstream target NF-κB.[48] Platelets from patients with type 2 diabetes show increased degranulation, adhesion, and aggregation of platelets,[49] which could be a result of an increased Orai1 expression and SOCE found in these platelets.[50] As SGK1 is strongly up-regulated in diabetic hyperglycemia,[17] we speculate that an increased stimulation of SGK1 in these patients could contribute to megakaryocytic NF-κB induction, stimulation of Orai1 expression resulting in enhanced SOCE, and increased activation-dependent responsiveness of their platelets. In view of the present observations, gain-of-function SGK1 polymorphisms could increase platelet responsiveness, thus predisposing the carriers to thrombotic complications. In a recent study, a common gain-of-function SGK1 gene variant indeed has been identified to be associated with ischemic stroke.[21]

As a result of the strong effect of SGK1 on Orai1 expression and the similarity between the phenotype of Orai1-deficient and SGK1-deficient platelets, it appears safe to conclude that the SGK1-dependent regulation of Orai1 protein abundance substantially contributes to SGK1-sensitive platelet function. However, it must be kept in mind that SGK1 regulates a variety of further carriers and channels, enzymes, and transcription factors,[17] which, at least in theory, could participate in the modulation of platelet function independently of regulating Orai1.

In conclusion, the present observations identify SGK1 as a novel transcriptional regulator of Orai1 in megakaryocytes which is at least partially effective through activation of NF-κB. Thus, SGK1-dependent Orai1 regulation in megakaryocytes can influence SOCE and activation-dependent Ca^{2+} entry as well as Ca^{2+}-dependent mechanisms, such as degranulation, aggregation, and thrombus formation in released platelets.

Authorship

Contribution: O.B. performed experiments, analyzed data, designed research, and wrote the manuscript; E.-M.S., P.M., T.S., S.T.T., M.E., C.L., E.S., and A.E. performed experiments and analyzed data; and A.E.M., D.K., M.G., and F.L. analyzed data, designed research, and wrote the manuscript.

Conflict-of-interest disclosure: The authors declare no competing financial interests.

Correspondence: Florian Lang, Department of Physiology, University of Tübingen, Gmelinstr 5, 72076 Tübingen, Germany; e-mail: florian.lang@uni-tuebingen.de.

References

1. Ruggeri ZM. Platelets in atherothrombosis. *Nat Med.* 2002;8(11):1227-1234.

2. Varga-Szabo D, Braun A, Nieswandt B. Calcium signaling in platelets. *J Thromb Haemost.* 2009;7(7):1057-1066.

3. Bergmeier W, Stefanini L. Novel molecules in calcium signaling in platelets. *J Thromb Haemost.* 2009;7(suppl 1):187-190.

4. Rink TJ, Sage SO. Calcium signaling in human platelets. *Annu Rev Physiol.* 1990;52:431-449.

5. Parekh AB. Store-operated CRAC channels: function in health and disease. *Nat Rev Drug Discov.* 2010;9(5):399-410.

6. Bergmeier W, Oh-hora M, McCarl CA, et al. R93W mutation in Orai1 causes impaired calcium influx in platelets. *Blood.* 2009;113(3):675-678.

7. Braun A, Varga-Szabo D, Kleinschnitz C, et al. Orai1 (CRACM1) is the platelet SOC channel and essential for pathological thrombus formation. *Blood.* 2009;113(9):2056-2063.

8. Varga-Szabo D, Braun A, Kleinschnitz C, et al. The calcium sensor STIM1 is an essential mediator of arterial thrombosis and ischemic brain infarction. *J Exp Med.* 2008;205(7):1583-1591.

9. Woodard GE, Lopez JJ, Jardin I, Salido GM, Rosado JA. TRPC3 regulates agonist-stimulated Ca2+ mobilization by mediating the interaction between type I inositol 1,4,5-trisphosphate receptor, RACK1, and Orai1. *J Biol Chem.* 2010;285(11):8045-8053.

10. Bogeski I, Kummerow C, Al Ansary D, et al. Differential redox regulation of ORAI ion channels: a mechanism to tune cellular calcium signaling. *Sci Signal.* 2010;3(115):ra24.

11. Pani B, Singh BB. Lipid rafts/caveolae as microdomains of calcium signaling. *Cell Calcium.* 2009;45(6):625-633.

12. Chen J, De S, Damron DS, et al. Impaired platelet responses to thrombin and collagen in AKT-1-deficient mice. *Blood.* 2004;104(6):1703-1710.

13. Jackson SP, Schoenwaelder SM, Goncalves I, et al. PI 3-kinase p110beta: a new target for antithrombotic therapy. *Nat Med.* 2005;11(5):507-514.

14. Gilio K, Munnix IC, Mangin P, et al. Non-redundant roles of phosphoinositide 3-kinase isoforms alpha and beta in glycoprotein VI-induced platelet signaling and thrombus formation. *J Biol Chem.* 2009;284(49):33750-33762.

15. Lian L, Wang Y, Draznin J, et al. The relative role of PLCbeta and PI3Kgamma in platelet activation. *Blood.* 2005;106(1):110-117.

16. Endo T, Kusakabe M, Sunadome K, Yamamoto T, Nishida E. The kinase SGK1 in the endoderm and mesoderm promotes ectodermal survival by down-regulating components of the death-inducing signaling complex. *Sci Signal.* 2011;4(156):ra2.

17. Lang F, Bohmer C, Palmada M, et al. (Patho-)physiological significance of the serum- and glucocorticoid-inducible kinase isoforms. *Physiol Rev.* 2006;86(4):1151-1178.

18. Sobiesiak M, Shumilina E, Lam RS, et al. Impaired mast cell activation in gene-targeted mice lacking the serum- and glucocorticoid-inducible kinase SGK1. *J Immunol.* 2009;183(7):4395-4402.

19. Eylenstein A, Gehring EM, Heise N, et al. Stimulation of Ca2+-channel Orai1/STIM1 by serum- and glucocorticoid-inducible kinase 1 (SGK1). *FASEB J.* 2011;25(6):2012-2021.

20. Busjahn A, Aydin A, Uhlmann R, et al. Serum- and glucocorticoid-regulated kinase (SGK1) gene and blood pressure. *Hypertension.* 2002;40(3):256-260.

21. Dahlberg J, Smith G, Norrving B, et al. Genetic variants in serum and glucocortocoid regulated kinase 1, a regulator of the epithelial sodium channel, are associated with ischaemic stroke. *J Hypertens.* 2011;29(5):884-889.

22. BelAiba RS, Djordjevic T, Bonello S, et al. The serum- and glucocorticoid-inducible kinase Sgk-1 is involved in pulmonary vascular remodeling: role in redox-sensitive regulation of tissue factor by thrombin. *Circ Res.* 2006;98(6):828-836.

23. Gawaz M, Langer H, May AE. Platelets in inflammation and atherogenesis. *J Clin Invest.* 2005;115(12):3378-3384.

24. Lang F, Klingel K, Wagner CA, et al. Deranged transcriptional regulation of cell-volume-sensitive kinase hSGK in diabetic nephropathy. *Proc Natl Acad Sci U S A.* 2000;97(14):8157-8162.

25. Wulff P, Vallon V, Huang DY, et al. Impaired renal Na(+) retention in the sgk1-knockout mouse. *J Clin Invest.* 2002;110(9):1263-1268.

26. Shivdasani RA, Schulze H. Culture, expansion, and differentiation of murine megakaryocytes. *Curr Protoc Immunol.* 2005;Chapter 22:Unit.

27. Ungerer M, Peluso M, Gillitzer A, et al. Generation of functional culture-derived platelets from CD34+ progenitor cells to study transgenes in the platelet environment. *Circ Res.* 2004;95(5):e36-e44.

28. Akbiyik F, Ray DM, Gettings KF, et al. Human bone marrow megakaryocytes and platelets express PPARgamma, and PPARgamma agonists blunt platelet release of CD40 ligand and thromboxanes. *Blood.* 2004;104(5):1361-1368.

29. Woulfe D, Jiang H, Morgans A, et al. Defects in secretion, aggregation, and thrombus formation in platelets from mice lacking Akt2. *J Clin Invest.* 2004;113(3):441-450.

30. Konopatskaya O, Gilio K, Harper MT, et al. PK-Calpha regulates platelet granule secretion and thrombus formation in mice. *J Clin Invest.* 2009; 119(2):399-407.

31. Authi KS. Orai1: a channel to safer antithrombotic therapy. *Blood.* 2009;113(9):1872-1873.

32. Dubois C, Panicot-Dubois L, Merrill-Skoloff G, Furie B, Furie BC. Glycoprotein VI-dependent and -independent pathways of thrombus formation in vivo. *Blood.* 2006;107(10):3902-3906.

33. Gilio K, van Kruchten R, Braun A, et al. Roles of platelet STIM1 and Orai1 in glycoprotein VI- and thrombin-dependent procoagulant activity and thrombus formation. *J Biol Chem.* 2010;285(31): 23629-23638.

34. Prakriya M, Feske S, Gwack Y, et al. Orai1 is an essential pore subunit of the CRAC channel. *Nature.* 2006;443(7108):230-233.

35. Zhang SL, Yu Y, Roos J, et al. STIM1 is a Ca2+ sensor that activates CRAC channels and migrates from the Ca2+ store to the plasma membrane. *Nature.* 2005;437(7060):902-905.

36. Ogura M, Morishima Y, Ohno R, et al. Establishment of a novel human megakaryoblastic leukemia cell line, MEG-01, with positive Philadelphia chromosome. *Blood.* 1985;66(6):1384-1392.

37. den Dekker E, Heemskerk JW, Gorter G, et al.

Cyclic AMP raises intracellular Ca(2+) in human megakaryocytes independent of protein kinase A. *Arterioscler Thromb Vasc Biol.* 2002;22(1):179-186.

38. Tolhurst G, Carter RN, Amisten S, et al. Expression profiling and electrophysiological studies suggest a major role for Orai1 in the store-operated Ca2+ influx pathway of platelets and megakaryocytes. *Platelets.* 2008;19(4):308-313.

39. Sherk AB, Frigo DE, Schnackenberg CG, et al. Development of a small-molecule serum- and glucocorticoid-regulated kinase-1 antagonist and its evaluation as a prostate cancer therapeutic. *Cancer Res.* 2008;68(18):7475-7483.

40. Leroy V, De Seigneux S, Agassiz V, et al. Aldosterone activates NF-kappaB in the collecting duct. *J Am Soc Nephrol.* 2009;20(1):131-144.

41. Zhang L, Cui R, Cheng X, Du J. Antiapoptotic effect of serum and glucocorticoid-inducible protein kinase is mediated by novel mechanism activating IκB kinase. *Cancer Res.* 2005;65(2):457-464.

42. Spinelli SL, Casey AE, Pollock SJ, et al. Platelets and megakaryocytes contain functional nuclear factor-kappaB. *Arterioscler Thromb Vasc Biol.* 2010;30(3):591-598.

43. Kim KW, Kim SH, Lee EY, et al. Extracellular signal-regulated kinase/90-KDA ribosomal S6 kinase/nuclear factor-kappa B pathway mediates

phorbol 12-myristate 13-acetate-induced megakaryocytic differentiation of K562 cells. *J Biol Chem.* 2001;276(16):13186-13191.

44. Greten FR, Arkan MC, Bollrath J, et al. NF-kappaB is a negative regulator of IL-1beta secretion as revealed by genetic and pharmacological inhibition of IKKbeta. *Cell.* 2007;130(5):918-931.

45. Karin M, Yamamoto Y, Wang QM. The IKK NF-kappa B system: a treasure trove for drug development. *Nat Rev Drug Discov.* 2004;3(1):17-26.

46. Myung J, Kim KB, Crews CM. The ubiquitin-proteasome pathway and proteasome inhibitors. *Med Res Rev.* 2001;21(4):245-273.

47. Karin M, Greten FR. NF-kappaB: linking inflammation and immunity to cancer development and progression. *Nat Rev Immunol.* 2005;5(10):749-759.

48. Baker RG, Hayden MS, Ghosh S. NF-kappaB, inflammation, and metabolic disease. *Cell Metab.* 2011;13(1):11-22.

49. Ferreira IA, Mocking AI, Feijge MA, et al. Platelet inhibition by insulin is absent in type 2 diabetes mellitus. *Arterioscler Thromb Vasc Biol.* 2006; 26(2):417-422.

50. Zbidi H, Lopez JJ, Amor NB, et al. Enhanced expression of STIM1/Orai1 and TRPC3 in platelets from patients with type 2 diabetes mellitus. *Blood Cells Mol Dis.* 2009;43(2):211-213.